JOURNAL OF BACTERIOLOGY, Oct. 2008, p. 6409–6418 Vol. 190, No. 19
0021-9193/08/$08.00+0 doi:10.1128/JB.00757-08

Formate-Dependent Autotrophic Growth in *Sinorhizobium meliloti*▽

Brad S. Pickering and Ivan J. Oresnik*

Department of Microbiology, University of Manitoba, Winnipeg, Manitoba, Canada

Received 28 May 2008/Accepted 19 July 2008

It was found that *S. meliloti* strain SmA818, which is cured of pSymA, could not grow on defined medium containing only formate and bicarbonate as carbon sources. Growth experiments showed that Rm1021 was capable of formate/bicarbonate-dependent growth, suggesting that it was capable of autotrophic-type growth. The annotated genome of *S. meliloti* Rm1021 contains three formate dehydrogenase genes. A systematic disruption of each of the three formate dehydrogenase genes, as well as the genes encoding determinants of the Calvin-Benson-Bassham, cycle was carried out to determine which of these determinants played a role in growth on this defined medium. The results showed that *S. meliloti* is capable of formate-dependent autotrophic growth. Formate-dependent autotrophic growth is dependent on the presence of the chromosomally located *fdsABCDG* operon, as well as the *cbb* operon carried by pSymB. Growth was also dependent on the presence of either of the two triose-phosphate isomerase genes (*tpiA* or *tpiB*) that are found in the genome. In addition, it was found that *fdoGHI* carried by pSymA encodes a formate dehydrogenase that allows Rm1021 to carry out formate-dependent respiration. Taken together, the data allow us to present a model of how *S. meliloti* can grow on defined medium containing only formate and bicarbonate as carbon sources.

Sinorhizobium meliloti is a gram-negative rhizobium that is capable of forming nodules on alfalfa, sweet clover, and trigonella. Bacterial infection occurs at the root hairs of the host plant, involving a signal exchange between the rhizobia and the plant (6, 55). Root hair curling encapsulates the bacteria, which subsequently travel through an infection thread and are finally released into plant cells, where they differentiate into bacteroids (24). In this environment, the bacteria reduce atmospheric nitrogen in exchange for nutrients and carbon compounds (37).

From the sequencing of its genome, it has become apparent that *S. meliloti* retains an array of genes that are capable of encoding enzymes for many metabolic pathways that allow the organism to scavenge energy from many different substrates (7, 23, 25). As a result of the whole-genome sequence data, greater effort has been made to address the functionality of many of the unknown open reading frames. Systems that have utilized the construction of either genetic deletions or genetic fusions of reporter genes have been developed for this purpose (15, 28, 40, 52).

Earlier efforts to uncover functionality associated with the megaplasmids in *S. meliloti* relied on the creation of precise deletions or plasmid-curing experiments (12, 45). These works showed that a number of carbon-catabolic loci, as well as transport systems, were associated with these plasmids (5, 12, 13, 45). It was also observed that an *S. meliloti* strain cured of pSymA had a reduced ability to respire formate (I. J. Oresnik, unpublished observation).

Formate is a ubiquitous compound in the environment. Many plants and bacterial species produce and excrete formate into their environments. The high negative reduction potential (−420 mV) of formate allows it to be a ready source of energy. For example, *Escherichia coli* is able to respire formate when grown under anaerobic conditions in the presence of nitrate as the terminal electron acceptor (18, 30, 31). Its oxidation results in the generation of a proton-motive force and the production of CO_2.

It has long been known that members of the *Rhizobiaceae* capable of forming nodules on legumes have an obligate need for CO_2 (27, 38). A variety of carboxylating enzymes needed for anapleurotic pathways have been shown to be present in these organisms (16), yet only *S. meliloti* and *Bradyrhizobium japonicum* have been shown to have ribulose bisphosphate carboxylase activity (39). To date, only *B. japonicum* has been shown to grow chemoautotrophically using H_2 gas as a sole source of electrons (27, 36). In contrast, *S. meliloti* has been shown to be unable to grow chemolithoautotrophically unless it is provided with a cosmid containing the hydrogen uptake genes from *B. japonicum* (34). *S. meliloti*, however, is capable of formate-dependent CO_2 fixation (39), but the molecular basis for this growth has never been elucidated. More recently, it has been shown that *S. meliloti* contains the necessary genetic components for the Calvin-Benson-Bassham pathway, as well as three annotated formate dehydrogenases (23, 32).

In this work, we characterize the ability of *S. meliloti* to grow on a medium containing only formate and bicarbonate as carbon sources. We show that two of the three annotated formate dehydrogenase gene clusters, *fdo* (consisting of sma0002, sma0005, and sma0007) and *fds* (consisting of smc02524, smc03086, smc03085, smc04444, smc02525, and smc02524), in *S. meliloti* affect formate-dependent growth. Moreover, we show that, in addition to the formate dehydrogenase genes, this growth is also dependent upon the *cbb* genes carried on pSymB.

MATERIALS AND METHODS

Bacterial strains, plasmids, media, and growth conditions. Bacterial strains, plasmids, and primers are listed in Tables 1 and 2. *S. meliloti* strains were grown at 30°C in either Luria-Bertani (LB) medium (42), Vincent's minimal medium

* Corresponding author. Mailing address: Department of Microbiology, University if Manitoba, Winnipeg, MB, R3T 2N2, Canada. Phone: (204) 474-7587. Fax: (204) 474-7603. E-mail: oresniki@cc.umanitoba.ca.

▽ Published ahead of print on 25 July 2008.

TABLE 1. Bacterial strains and plasmids

Strain or plasmid	Genotype or phenotype	Reference or source
Strains		
S. meliloti		
Rm1021	SU47 *str-21* Sm^r	41
Rm2011	Sm^r wild type of RCR2011 (SU47)	10
SmA818	Rm2011; pSymA cured	45
SRmA330	Rm1021; *fdoG*::pKnock-Gm^r	This work
SRmA402	Rm1021; sma0478::pKan^r	This work
SRmA411	Rm1021; *fdsA*::pKnock-Tc^r	This work
SRmA442	Rm1021; *cah*::pKnock-Gm^r	This work
SRmA493	*fdsA fdoGHI* ΦM12(SRmA411) → SRmA330[a] Gm^r Tc^r	This work
SRmA495	sma0478 *fdsA* ΦM12(SRmA402) → SRmA411 Nm^r Tc^r	This work
SRmA497	*fdoG* sma0478 ΦM12(SRmA330) → SRmA402 Gm^r Nm^r	This work
SRmA571	*fdoG* sma0478 *fdsA* ΦM12(SRmA411) → SRmA497 Gm^r Nm^r Tc^r	This work
SRmA580	Rm1021; *cbbF1*::Kan^r	This work
E. coli		
MM294A	*pro-82 thi-1 hsdR17 supE44*	22
S17-1	*recA* derivative of MM294A with integrated RP4-2 (Tc::Mu::Km::Tn*7*)	54
MT607	MM294A; *recA56*	22
MT616	MT607(pRK600)	22
DH5α	λ^- ϕ80d*lacZ*°M15 °(*lacZYA-argF*)*U169 recA1 endA1 hsdR17*(r_K^- m_K^-) *supE44 thi-1 gyrA relA1*	26
DH5αλpir	λpir lysogen of DH5α	28
Plasmids		
pBluescriptII SK	Cloning vector; ColE1 *oriV* Ap^r	Stratagene
pRK600	pRK2013 *npt*::Tn*9* Cm^r	22
pRK415	Tc^r IncP broad-host-range cloning vector	33
pPH1JI	IncP plasmid; Gm^r	8
pKnock-Tc	Suicide vector for insertional mutagenesis; R6K *ori* RP4 *oriT* Tc^r	2
pKnock-Gm	Suicide vector for insertional mutagenesis; R6K *ori* RP4 *oriT* Gm^r	2
pKan	pK*NOCK*-Gm^r replaced with Km^r	This work
pBP1	*fdoG* internal fragment in pKnock-Gm	This work
pBP3	*fdsA* internal fragment in pBlueScript	This work
pBP6	*cbbF* fragment in pBlueScript	This work
pBP9	sma0478 internal fragment in pKnock-Gm	This work
pBP13	sma0478 internal fragment in pKan	This work
pBP15	*fdsA* internal fragment in pKnock-Tc	This work
pBP19	*cah* internal fragment in pKnock-Gm	This work
pBP20	Kan^r cassette cloned into *cbbF* fragment in pBP6	This work
pBP32	*cbbF*::Kan^r from pBP20 cloned into pRK415	This work
pMM22	Kan^r fragment cloned as a SmaI fragment into pBlueScript	This work

[a] SRmA493 was constructed by ΦM12 transduction by transducing Tc^r from SRmA411 into SRmA330. The transductants were subsequently screened for Gm^r.

(VMM) (59), or *Rhizobium* minimal medium (RMM) (9). Generally, carbon sources were filter sterilized prior to use and were added to defined media to a final concentration of 15 mM. To grow strains in defined medium containing only formate or bicarbonate as carbon sources, the strains were first grown in LB medium supplemented with 15 mM sodium formate and subsequently subcultured into VMM or RMM containing 60 mM sodium formate and 5 mM sodium bicarbonate. This medium was routinely supplemented with biotin and methionine (5 μg ml^{-1} each), as previously suggested (60); in addition, sodium selenate and sodium molybdate were added to a final concentration of 20 μM. All cultures grown in this manner were streaked for purity. When required, the final concentrations of antibiotics were as follows: tetracycline (Tc), 5 μg ml^{-1}; gentamicin (Gm), 60 μg ml^{-1}; neomycin (Nm), 100 μg ml^{-1}; streptomycin (Sm), 200 μg ml^{-1}; kanamycin (Kan), 40 μg ml^{-1}; ampicillin (Ap), 200 μg ml^{-1}.

TABLE 2. Primers used in this work

No.	Primer name	Sequence (5′→3′)
1	fdsAFwd	TGAAGCAGGCGCGTTTCG
2	fdsARvs	GCTGTGATGGGGCTCGG
3	fdoGFwd	ATATGAATTCATCATTCACATCGAAGGCG
4	fdoGRvs	ATATGAATTCAGCAGATTCCAGACACAAC
5	sma0478Fwd	ATATGAATTCAGGTCGAAGGTTCG
6	sma0478Rvs	ATATGAATTCATGCAGCGCTGCGGCC
7	cbbFwd	ATATGGATCCCGGCCTCGTCGTGCAC
8	cbbRvs	ATATGATATCTGTCAGGCGCGACTCTC

Genetic manipulations. Conjugations of *S. meliloti* and *E. coli* were carried out as previously described (49). Mutants that were constructed and recombined into the genome of *S. meliloti* were retransduced into Rm1021 prior to experimental use, as previously described (21).

DNA manipulations, mutant construction, and Southern analysis. Standard techniques were used for plasmid isolation, restriction enzyme digestion, and agarose gel electrophoresis (51). Mutations were routinely verified by Southern blot analysis, as previously described (14).

The vector pKan was constructed by modification of pKnock-Gm. Briefly, pKnock-Gm, containing an internal EcoRV site in the gentamicin cassette, was restricted with EcoRV and blunt-end cloned with a SmaI kanamycin cassette obtained from pMM22. The final construct was verified by restriction and designated pKan.

To construct a strain carrying a mutation in *fdsA* (smc04444), a 2,020-bp internal fragment of *fdsA* was PCR amplified using primers 1 and 2 (Table 2) from Rm1021 genomic DNA, isolated, digested with EcoRI, and cloned into pBluescript II SK, yielding pBP3. pBP3 was digested with KpnI and PstI to yield a 1,023-bp fragment, subsequently cloned into pKnock-Tc (2), and transformed into DH5αλpir, yielding pBP15 (Table 1). pB15 was mobilized into Rm1021 with MT616, and single-crossover recombinants were selected as previously described (49). The resultant strain was verified by Southern blot analysis and named SRmA411 (Table 1).

Similarly, an *fdoG* (sma0002) mutation was constructed by utilizing primers 3 and 4 (Table 2). The 869-bp fragment generated from these primers was restricted with EcoRI, gel isolated, and cloned into pKnock-Gm, yielding pBP1 (Table 1), which was subsequently conjugated and recombined into Rm1021. The resultant strain was verified by Southern blot analysis and named SRmA330 (Table 1).

A fragment internal to sma0478 was PCR amplified from genomic DNA using primers 5 and 6 (Table 2) to yield a 1,050-bp fragment. This fragment was digested with BamHI/PstI, and the resulting 750-bp product was gel isolated and cloned into pKan to give pBP14. pBP14 was transformed into DH5αλpir, verified by restriction, and conjugated into Rm1021. This construct was conjugated into the wild type, and Sm^r Nm^r single-crossover recombinants were selected. The resultant strain was verified by Southern blot analysis and designated SRmA411.

To construct a *cbb* mutation, primers 7 and 8 were used to amplify a portion of *cbbF*. The fragment isolated was restricted with BamHI/EcoRV and cloned into pBlueScript, yielding pBP6. A Kan^r cassette was cut as a SmaI fragment from pMM22, gel isolated, and ligated into pBP6, which was digested with StuI, yielding pBP20. The Kan^r cassette and the flanking DNA (from *cbbF*) were removed as a BamHI/EcoRV fragment from pBP20 and recloned into pRK415, yielding pBP32 (Table 1). pBP32 was conjugated into Rm1021, and allelic exchange was carried out using pPH1JI as previously described (46). The resultant strain, SRmA580, was verified by amplifying the insertion junctions and sequencing the PCR products.

Whole-cell CO_2 incorporation and formate uptake. To assay carbon fixation, cells were grown in RMM containing 60 mM sodium formate and 5 mM sodium bicarbonate to an optical density at 600 nm of approximately 0.3. The cells were pelleted, washed twice with phosphate buffer, and finally resuspended in 10 ml of buffer. Incorporation was initiated by the addition of $Na_2{}^{14}CO_3$. Aliquots of 1 ml were taken at 0, 2, 5, 10, 15, 30, 45, and 60 min; quenched with perchloric acid (10% [vol/vol] final concentration); and allowed to degas overnight. Acid-stable counts were determined using a Beckman LS 6500 liquid scintillation spectrophotometer and were 3 orders of magnitude above those of dead-cell controls. Linear portions of the data were used to determine fixation rates, and incorporation was normalized to the total cell protein, measured using an enhanced Lowry protein assay (56).

Uptake of formate was carried out essentially as previously described (47). Cells were grown as described above, and assays were initiated with the addition of $Na^{14}COOH$. Some assays were allowed to continue for over 15 min. Incorporation and normalization of data were as described above.

Native gel formate dehydrogenase assay. Cells were grown in either complex or defined medium, depending upon the experiment. The preparation of cell extracts was carried out as previously described (44, 47). Native polyacrylamide gel electrophoresis (PAGE) gels were run as previously described (45). The PAGE gels were developed using a *p*-nitroblue tetrazolium (*p*-NBT)-based formate dehydrogenase stain (35). Samples were stained with and without both formate and NAD^+ to determine the specificities of the activity stains.

Determination of oxygen consumption. Cells were grown to an optical density at 600 nm of at least 0.20. The cultures were washed twice and resuspended in a phosphate buffer (containing K_2HPO_4, KH_2PO_4, and KNO_3, pH 7). Oxygen consumption was measured using a Gilson-Clark-type oxygen electrode. Formate-dependent oxygen consumption rates were determined by subtracting the endogenous rates measured prior to the addition of sodium formate from the measured rates following the addition of formate. To ensure that cells were coupled, each assay was concluded by the addition of 2 μM carbonyl cyanide *m*-chlorophenylhydrazone. Oxygen consumption was normalized to the total cell protein, measured using an enhanced Lowry protein assay (56).

Phylogenetic analysis. Phylogenetic analysis was carried out essentially as previously described (50). Briefly, sequences were selected on the basis of BLASTP scores (3), aligned using CLUSTAL-X (57), and analyzed using PHYLIP version 3.6a (19, 20). The resulting distance matrix was used to construct a phylogenetic tree and was evaluated using a bootstrap procedure (SEQBOOT; 1,000 replicates).

RESULTS

Formate-dependent chemoautotrophic growth. The generation of SmA818, a strain cured of the megaplasmid pSymA, allowed the initial identification of a number of pSymA-associated catabolic phenotypes prior to the release of the completed sequence of Rm1021 (45). Many of the putative phenotypes that were observed using BioLog plates, however, were difficult to confirm because of the difficulty in growing the wild-type strain well enough using the identified carbon or nitrogen source. One such observed phenotype was the inability of SmA818 to reduce the indicator dye found within the BioLog plates in the presence of formate as a sole carbon source.

Formate is a one-carbon carboxylic acid. Formate can be oxidized to CO_2, and the energy can be used to generate a proton-motive force that in some bacteria can also be used to generate reductant. The resultant CO_2 is either reduced or released as a waste product. In other bacteria, formate can be reduced directly and used as a carbon source. The availability of the genomic sequence of Rm1021 provided the opportunity to systematically pursue the observed phenotype of SmA818 grown in the presence of formate. As an initial experiment, we set out to grow Rm1021 in a defined medium with formate as a carbon source.

Wild-type Rm1021 (also Rm2011) and SmA818 were grown on VMM supplemented with 60 mM formate. Since Rm1021 has known deficiencies with respect to biotin and cobalt (60), the medium was supplemented with these, as well as a mixture of trace metals, because many of the enzymes that utilize formate require trace metals (18). It was also possible that formate might be utilized only as an electron source and that the carbon source would be derived from the product of formate oxidation, CO_2. To alleviate the possibility that growth would not be observed because of low dissolved CO_2 concentrations, bicarbonate was added to increase the amount of dissolved CO_2, thus allowing the possibility of autotrophic growth.

The growth curves clearly showed that Rm1021 does have the capability of growing on a defined medium with formate and bicarbonate as the only sources of carbon (Fig. 1). Growth was dependent upon the presence of bicarbonate, as well as formate. Omission of formate from the medium resulted in Rm1021 growth curves that resembled those of SmA818, characterized by a single doubling following subculture into formate/bicarbonate-containing medium. To determine the effect of reduced levels of bicarbonate, Rm1021 was grown without the addition of bicarbonate to the medium. Growth was greatly decreased and increased only slightly over time compared to the control (data not shown). These results are consistent with the premise that the CO_2 concentration within the growth medium slowly increased as formate was oxidized to CO_2.

To control for growth that might have been due to carryover of nutrients from the starter culture, Rm1021 was also tested for growth on the base medium without formate or bicarbonate and only the amount of complex medium that would be introduced during subculture. The growth of Rm1021 that occurred under these conditions resembled that of SmA818 (data not shown). Interestingly, if an amount of complex medium equivalent to the amount that was used for the initial

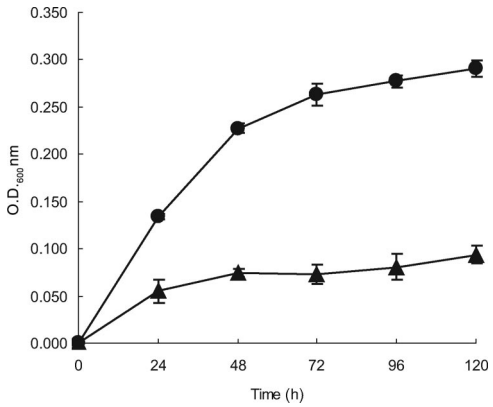

FIG. 1. Formate-dependent autotrophic growth. Growth curves of *S. meliloti* strains grown in VMM containing 60 mM formate and 5 mM bicarbonate. Rm1021, ●; SmA818, ▲. The data were pooled from four independent experiments; standard deviations are shown. OD_{600}, optical density at 600 nm.

subculture was added when wild-type cells reached stationary phase, growth would resume. This suggests that the complex medium must contain some vitamin or nutrient that is not found in our defined medium. The elucidation of this compound(s) was not pursued.

pSymA contains an inducible NAD^+ formate dehydrogenase activity. Nondenaturing protein gels incubated with substrates that lead to the visualization of specific enzyme activities has long been used as a tool in population genetics studies to quantitatively score loci in *Rhizobium* (17, 53). This technique has also been used to characterize mutations (4, 11, 13, 45). Since the genome of *S. meliloti* is predicted to contain multiple formate dehydrogenase genes, it was reasoned that this technique would allow us to distinguish the different formate dehydrogenase activities.

The annotated sequence of *fdoGHI* suggests that these genes encode a periplasmic formate dehydrogenase complex

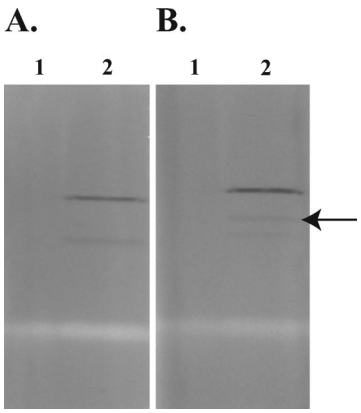

FIG. 2. Native PAGE formate dehydrogenase activity. *S. meliloti* strains were grown in defined medium containing 5 mM bicarbonate and 60 mM formate. Gels were stained for dehydrogenase activity with either the absence of formate and the presence of NAD^+ (A) or the absence of NAD and the presence of formate (B). Lanes 1, SmA818; lanes 2, Rm1021. The arrow indicates an activity band that is formate dependent and NAD^+ independent. Equivalent amounts of protein were loaded in all lanes.

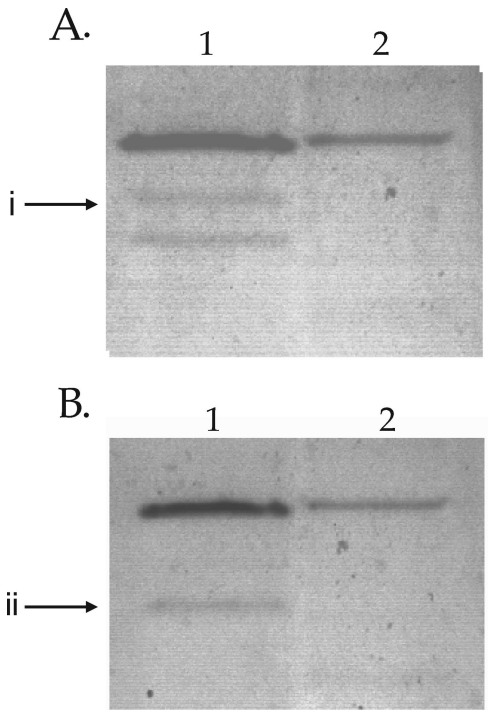

FIG. 3. Native PAGE gels depicting formate-inducible enzyme activity. Shown are extracts from *S. meliloti* Rm1021 grown in defined medium containing either 5 mM bicarbonate and 60 mM formate (lanes 1) or 5 mM bicarbonate and 15 mM glucose (lanes 2). (A) Stained in the presence of 30 mM formate and in the absence of NAD^+. (B) Stained in the presence of NAD^+ and the absence of formate. i, a formate-dependent activity band that was present when the bacteria were grown with formate; ii, an activity band that was dependent upon growth in formate but was not dependent on the presence of either formate or NAD^+. Note that extracts from glucose-grown cells contained two times the amount of protein in formate grown cells.

that is NAD^+ independent (7). To test the hypothesis that SmA818 lacked NAD^+-independent formate dehydrogenase activity, SmA818 was cultured on defined medium containing formate/bicarbonate. Since SmA818 showed some limited growth in this medium, cells from approximately 2 liters of culture were pooled to provide enough bacterial cells to make cell extracts. Equal amounts of SmA818 and Rm1021 proteins were loaded onto nondenaturing polyacrylamide gels, run, and stained in the presence or absence of NAD^+ and formate in an effort to show functionality.

Consistent with the gene annotation, the results showed that Rm1021 contained a formate-dependent, NAD^+-independent activity band that was absent in SmA818 (Fig. 2). To determine if this formate-dependent, NAD^+-independent activity was constitutive or inducible, extracts from Rm1021 that were grown with either glucose or formate were compared. The presence of this activity band was dependent upon being grown in the presence of formate and was not seen in cell extracts from glucose-grown cells (Fig. 3). Moreover, this activity band was absent in cell extracts from cells grown on complex media, such as LB or tryptone-yeast extract medium, but was present if formate was added to the medium (data not shown). Together, these data suggest that the band of formate dehydro-

genase activity being visualized is inducible by the presence of formate. Interestingly, we noted that a second activity band was detectable (Fig. 3). This activity band was not dependent on the presence of either formate or NAD^+ and was detectable when the cells were grown in the presence of formate (Fig. 3).

The *S. meliloti* Rm1021 genome contains genes encoding three probable formate dehydrogenases. A text search of the descriptions of the annotated open reading frames in Rm1021 revealed that genes for three putative formate dehydrogenases might exist in the *S. meliloti* genome. Two sets of genes, *fdoGHI* and sma0478, are carried on the megaplasmid pSymA. The third, *fdsABCDG*, is located on the chromosome.

FdoGHI consists of three subunits. The alpha subunit (FdoG) contains the active site, and the beta subunit (FdoH) contains Fe-S clusters and is involved in electron transfer from the active-site subunit to the gamma subunit (FdoI), which is an integral membrane protein that can donate electrons to quinones (31). The alpha subunit is also predicted to contain a molybdopterin cofactor, as well as an in-frame opal codon that is used for selenocysteine incorporation into the active site (7). Many of these types of formate dehydrogenase enzymes are targeted to the periplasm (29). We noted that *fdoG* also contains a putative twin-arginine leader and the only codon in the entire *S. meliloti* genome for selenocysteine (7). Interestingly, the genes annotated as encoding selenocysteine biosynthesis lie immediately adjacent to the *fdoGHI* operon (23).

The other formate dehydrogenase gene found on pSymA, sma0478, is annotated as encoding a probable formate dehydrogenase, and a simple BLASTP search revealed that it also appeared moderately similar to hydroxy-acid dehydrogenases. This gene is not found in any other sequenced member of the *Rhizobiaceae*.

The chromosomal formate dehydrogenase, encoded by *fdsABCDG*, is conserved among other *Rhizobiaceae*. It is predicted to contain a molybdopterin cofactor and to be NAD^+ dependent and may reside on the cytosolic face of the inner membrane.

Since formate dehydrogenases have not been previously characterized in *S. meliloti*, insertional mutants were constructed in each of the putative formate dehydrogenases to assess what roles they may have in growing in defined medium containing only formate and bicarbonate as sole carbon sources (Table 1). From these, three double formate dehydrogenase mutants, SRmA493, SRmA495, and SRmA497, containing *fdsA*/*fdoG*, sma0478/*fdsA*, and *fdoG*/sma0478, respectively, were constructed by transduction. Similarly, SRmA571 was constructed to be mutated for each of the predicted formate dehydrogenase alleles. Because it appeared that Rm1021 was growing autotrophically (Fig. 1), the *cbb* genes present on pSymB were also mutated so that it could be unambiguously determined whether *S. meliloti* was growing using the Calvin-Benson cycle.

Growth using formate and bicarbonate is dependent upon the Calvin-Benson cycle. Growth experiments clearly showed that SRmA330 (containing an *fdoGHI* mutation) and SRmA402 (containing an sma0478 mutation) appeared to grow very similarly to Rm1021 (Fig. 4A). SRmA411 (containing an *fdsA* mutation), however, did not show any growth on this medium (Fig. 4A). Similarly, SRmA580 (containing a *cbbF*

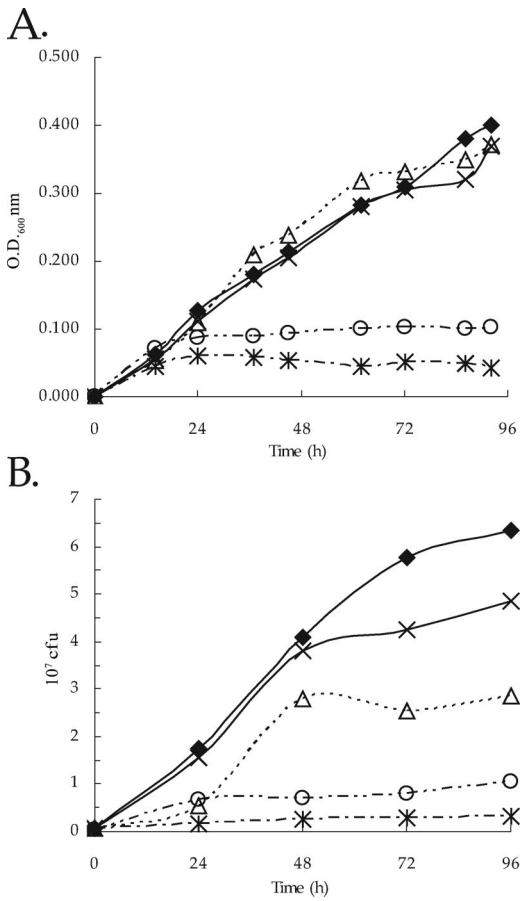

FIG. 4. Growth and viability of *S. meliloti* in defined medium. (A) Growth curve for *S. meliloti* strains grown in RMM containing 60 mM formate and 5 mM bicarbonate. (B) Viability of cultures at each time point. The data represent three independent experiments; standard deviations are shown. ◆, Rm1021; △, SRmA330; ×, SRmA402; ∗, SRmA411; ○, SRmA580. OD_{600}, optical density at 600 nm.

mutation) did not grow. These data suggest that growth on defined medium containing formate and bicarbonate is dependent upon the Calvin-Benson cycle genes and the chromosomally located *fds* locus. Surprisingly, a mutation in either the *fdoGHI* locus or the sma0478 locus did not appear to have the same phenotype as SmA818 (Fig. 4A). Also, strain SRmA497 (containing *fdoGHI* and sma0478 mutations) did not have the same growth phenotype as SmA818 (data not shown).

Measurement of growth using optical density assumes a direct correlation between the optical density and cell viability. Since there was a discrepancy between the growth of SmA818 and our working hypothesis that *fdoGHI* and/or sma0478 would be necessary for growth on this medium, we wished to test whether the culture optical density was correlated with cell viability. To carry this out, aliquots were taken at each time point and plated for viability. The results showed that the viability results appeared to be mostly congruent with those in which optical density was used as a measure of growth (Fig. 4). In most experiments, a strain carrying a mutation in sma0478 was either very close to or indistinguishable from the wild type (Fig. 4B and data not shown). SRmA330 (containing an *fdoGHI* mutation) consistently showed viable counts that were

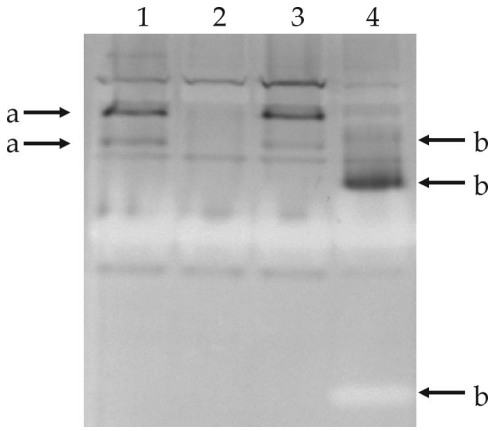

FIG. 5. Native PAGE analysis of formate dehydrogenase mutants. Extracts from *S. meliloti* strains were grown in LB medium supplemented with 60 mM sodium formate. Gels were stained for dehydrogenase activity in the presence of formate and NAD^+. Lane 1, Rm1021; lane 2, SRmA330 (*fdoG*::pKnock-Gm); lane 3, SRmA402 (sma0478::p*Kan*); lane 4, SRmA411 (*fdsA*::pKnock-Tc). a, *fdoG*-dependent activity bands; b, *fdsA*-dependent activity bands. Equal amounts of protein were loaded in all lanes.

half of those from Rm1021. Moreover, the colonies of SRmA330 formed more slowly when taken from the defined broth medium and plated onto LB medium. Taken together, these data suggest that *fdoGHI* does play a role in growth on defined medium containing only formate and bicarbonate as carbon sources but that its role is dispensable (Fig. 4B).

Organisms using the Calvin-Benson cycle reduce CO_2 utilizing ribulose 1,5-bisphosphate carboxylase/oxygenase. The cell removes carbon from this cycle as glyceraldehyde 3-phosphate. Glyceraldehyde 3-phosphate is subsequently isomerized by triose phosphate isomerase to dihydroxyacetone phosphate, and a hexose is synthesized via an aldolase reaction, yielding fructose 1,6-bisphosphate. It has recently been shown that *S. meliloti* contains two triose phosphate isomerases (48). It has been shown that *tpiA* plays a role in central metabolic metabolism (48), whereas *tpiB* appears to be necessary for erythritol catabolism in *S. meliloti* and *Rhizobium leguminosarum* (48, 61). Although TpiB activity appears to be specifically induced by erythritol, there appears to be enough residual activity from TpiB so that only a strain carrying both a *tpiA* and a *tpiB* mutation was unable to grow on carbon sources that necessitated the use of gluconeogenesis (48). It was reasoned that if *S. meliloti* growth was dependent upon CO_2 fixation, strains carrying either a *tpiA* mutation or a *tpiB* mutation would be capable of growing on defined medium with formate and bicarbonate as sole carbon sources but a strain carrying both mutations would be unable to grow. This hypothesis was tested, and it was found that strains carrying either *tpiA* or *tpiB* grew in a manner similar to the wild type, whereas a double *tpiA-tpiB* mutant had the same growth characteristics as SRmA580 (*cbbF*), strongly suggesting that *S. meliloti* does utilize the Calvin-Benson cycle for growth on defined medium that contains only formate and bicarbonate as carbon sources (data not shown).

***fdoGHI* and *fdsABCDG* mutants lack formate dehydrogenase activity.** Since it was not possible to grow all the formate dehydrogenase insertional mutants on defined medium with formate and bicarbonate (Fig. 4) but we had evidence that formate dehydrogenase activity was inducible (Fig. 3), and there is evidence for multiple-enzyme complexes having similar enzymatic activities, it was reasoned that the most straightforward method to separate these activities would be to carry out activity stains on induced extracts of the mutants and compare these to the wild type (Fig. 5). The results clearly showed that SRmA330 (*fdoG*) and SRmA411 (*fdsA*) zymograms differed from that of Rm1021. In SRmA330, two bands of activity (Fig. 5, bands a) that were NAD^+ independent were missing, whereas the pattern yielded by SRmA411 (Fig. 5, bands b) was different and complex, suggesting that the *fdsABCDG* locus is correlated with formate dehydrogenase activity. The pattern yielded by an extract of SRmA402 (sma0478) did not show any discernible differences from that of the wild type.

We also noted the appearance of achromatic bands associated with the *fdsABCDG* mutant (Fig. 5). Since the activity stain works on the principle that electrons from dehydrogenases reduce NBT, forming a blue precipitate at the point of activity, an achromatic band is often associated with enzymes that use reduced NBT as a provider of electrons. It is not clear from our data whether these achromatic bands could be due to the formation of incomplete formate dehydrogenase complexes or whether they might be due to other regulatory changes that might occur in the absence of *fdsABCDG.* These may lead to the expression of other genes that encode enzymes, such as superoxide dismutases, that are noted for this type of staining pattern (45).

CO_2 incorporation activity is reduced in an *fdoGHI* mutant. Two carbon sources are available in our defined growth medium, formate and bicarbonate. To try to resolve whether *S. meliloti* grew by using formate or CO_2, Rm1021 was assayed for incorporation of either formate or bicarbonate into an acid-stable product. Incubation of Rm1021 with labeled formate during a 15-min assay resulted in amounts of incorporation that were barely over the level that was found with the dead-cell controls (data not shown). Incubation of Rm1021 with $Na^{14}CO_3$ yielded radiolabel incorporation that showed saturation (Table 3). In contrast, SRmA580 (*cbbF*) had rates that were less than one-fifth that of the wild type (Table 3). These data show that the majority of the carbon incorporated from our defined medium is dependent upon the presence of the Calvin-Benson cycle.

To determine if the products encoded by either *fdoGHI* or sma0478 play roles in carbon fixation, whole cells carrying

TABLE 3. Acid-stable CO_2 fixation[a]

Strain	Relevant genotype	Rate (nmol/min/mg protein)[b]	% of wild type
Rm1021	Wild type	54.2	100
SRmA330	*fdoGHI*	21.3	39.4
SRmA402	sma0487	52.2	96.3
SRmA411	*fdsABC*	ND	ND
SRmA580	*cbbF*	9.4	17.4

[a] The table represents the data from a single experiment; the numbers represent the averages of two independent cultures for each strain. The experiment was repeated three times, showing consistent results.
[b] The rates are directly compared to that of Rm1021. ND, not determined.

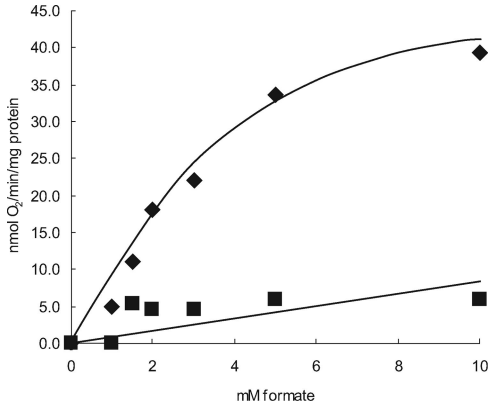

FIG. 6. Oxygen consumption is FdoG dependent. Cells were grown in RMM containing 60 mM formate and 5 mM bicarbonate. ◆, Rm1021; ■, SRmA330 (*fdoG*). Note that endogenous respiration rates were subtracted from both the wild type and SRmA330.

these mutations were grown with formate and bicarbonate and were also assayed for $^{14}CO_2$ incorporation. Whereas SRmA402 incorporation rates were identical to those of the wild type, the rates of CO_2 incorporation in SRmA330 were consistently less than half those of the wild type. This is consistent with the hypothesis that *fdoGHI* does indeed play a role in formate-dependent autotrophic growth but that its presence is not essential (Table 3).

Formate-dependent oxygen consumption is dependent on *fdoGHI*. Based on the annotation of *fdoGHI*, as well as simple bioinformatic searches, it was predicted that FdoGHI should form a complex that is capable of oxidizing formate and donating the electrons directly to the ubiquinol and subsequently to a terminal oxidase, leading to formate-dependent oxygen consumption. To directly test the functionality of FdoGHI, it was hypothesized that Rm1021 should be capable of formate-dependent oxygen reduction, whereas an *fdoGHI* mutant should be impaired in this ability.

To verify this, cells were grown in minimal media containing formate and bicarbonate as their sole carbon sources and tested for formate-dependent oxygen consumption. Experiments carried out with the wild type showed that *S. meliloti* did display formate-dependent respiration, and the whole-cell kanamycin level for formate was approximately 2.4 mM (Fig. 6). It was found that oxygen consumption was completely abolished in a strain carrying an *fdoGHI* mutation (Fig. 6). Immediately downstream of *fdoGHI*, and presumably within the same operon, are the genes *fdhE*, *selA*, and *selB*. Whereas SelA and SelB are likely involved in the biosynthesis of the selenocysteine necessary for FdoG activity (7), FdhE has been identified as a maturation protein likely involved in FdoGHI maturation (58). Interestingly, unlike *E. coli*, in which an *fdhE* mutation completely blocks formate dehydrogenase activity (1), a strain carrying a deletion of the *fdhE* open reading frame so that transcription of *selAB* was not affected still showed formate-dependent oxygen consumption, albeit at reduced rates (B. S. Pickering and I. J. Oresnik, unpublished data). These results suggest that the FdoGHI complex does play a direct role in oxidizing formate and that the electrons are donated to the electron transport chain and play a role in generating a proton-motive force across the cell membrane.

***fdoGHI* is not found in other *Rhizobium* species.** A BLASTP search revealed that the presence of *fdoGHI* is not common within the alphaproteobacteria, whereas the *fdsABCDG* genes are found in every member of the *Rhizobiaceae* that has been sequenced. To better assess *fdoGHI*, a phylogeny of FdoG was carried out with the top BLAST hits. The results clearly showed that FdoG is found in only four other alphaproteobacteria: *Xanthobacter autotrophicus*, *Azorhizobium caulinodans*, *Ochrobactrum anthropi*, and *Paracoccus denitrificans*. The FdoG found in *S. meliloti* is most closely related to that of the alphaproteobacterial species *P. denitrificans*. Interestingly, the genes *fdoGHI* are usually associated with either beta- or gammaproteobacterial species that are usually facultative anaerobes. The phylogenetic data strongly supports the idea that *fdoGHI* were acquired by a lateral gene transfer event from either a beta- or gammaproteobacterium. Strikingly, the genes for *fdoGHI*, as well as the associated genes for selenocysteine biosynthesis, are not found in the closely related species *Sinorhizobium medicae*. It may be noteworthy that *S. medicae* strain WSM419 is capable of formate-dependent autotrophic growth (data not shown).

DISCUSSION

The basic premise for carrying out this work was to investigate which of the formate dehydrogenase genes on pSymA were responsible for a delayed formate respiration phenotype that was observed with a strain that was devoid of pSymA. It was reasoned that this information would provide functional evidence that would increase our physiological understanding of the sequenced *S. meliloti* strain Rm1021. The data presented show that Rm1021 can grow on a formate bicarbonate defined medium (Fig. 1). Moreover, we have shown that this growth is not solely dependent upon the presence of pSymA but on genetic determinants that are found on both the chromosome and pSymB (Table 3 and Fig. 4A).

Taken together, the data provide sufficient evidence to allow us to construct a model of how *S. meliloti* can grow by utilizing only formate and bicarbonate (Fig. 7). Uptake assays clearly showed that the rates of formate uptake are consistent with this compound entering into the cell by diffusion and that very little carbon is assimilated into cell material (data not shown). In contrast, labeling experiments with bicarbonate showed that carbon incorporation occurs rapidly and is dependent upon the *cbb* operon found on pSymB (Table 3). In addition to the genes found on pSymB, growth was also dependent upon the presence of *tpiA* and *tpiB*. This observation is consistent with our understanding of how carbon is taken from the Calvin-Benson-Bassham cycle and utilized for gluconeogenesis. These data are all consistent with the hypothesis that the carbon source for growth on our defined formate-bicarbonate medium is CO_2. In some organisms, the uptake of bicarbonate has been shown to be an active process (43). It may be a noteworthy observation that an ABC transporter is found in close proximity to the *cbb* operon on pSymB.

Whereas SmA818 was unable to grow on our defined medium, growth experiments with strains carrying defined mutations in each of the annotated formate dehydrogenase genes

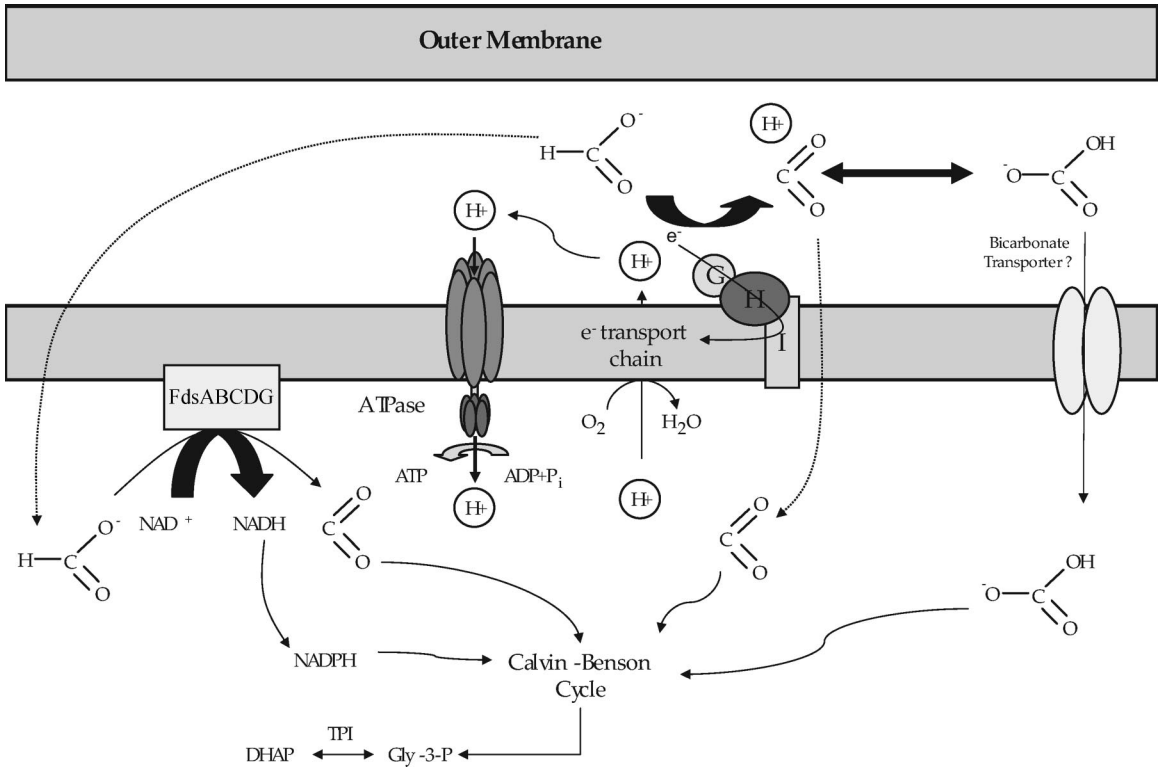

FIG. 7. Model for formate-dependent autotrophic growth in *S. meliloti* Rm1021. See the text for details.

clearly showed that *fdsABCDG* is essential for growth on our formate-bicarbonate defined medium whereas *fdoGHI* plays a nonessential role (Fig. 4 and Table 3). It was shown, however, that FdoGHI is responsible for formate-dependent oxygen consumption (Fig. 6). Although it is theoretically possible to produce reductant directly from formate using FdoGHI, our data suggest that the primary source for reductant using our growth conditions must be provided by FdsABCDG, since any strains that carried a mutation in *fdsA* did not grow on our defined medium (Fig. 4). FdoGHI must therefore contribute to the overall energetics of the cell by contributing to the proton-motive force (Fig. 6). These data are also consistent with the decreased rates of CO_2 fixation and lower viability observed in SRmA330 (Fig. 4B and Table 3). We noted that *S. medicae* strain WSM419 was also capable of formate-dependent autotrophic growth, although it does not carry *fdoGHI* and the associated genes for the biosynthesis of selenocysteine (data not shown).

Clearly there are determinants on pSymA that affect growth in a defined medium containing only formate and bicarbonate. We noted that a carbonic anhydrase (*cah*; sma0045) gene is also found in close proximity to *fdoGHI*. Defined mutations of this gene did not affect rates of carbon fixation (data not shown). Also, we were unable to ascribe any function that was related to formate utilization to sma0478. It is currently unclear whether the inability of SmA818 to grow in this defined medium is a direct affect of a single locus on pSymA or if it is an effect of a number of independent loci that cumulatively give rise to the inability to grow. These questions are currently unresolved.

The presence of *fdoGHI* in *S. meliloti* is curious. To date, this complex has not been found in any other sequenced member of the genus *Rhizobium* and very few other alphaproteobacteria. As might be expected, all of the FdoG proteins within the alphaproteobacteria appear to be from a distinct branch on our phylogenetic tree (data not shown). With a greater number of the *Rhizobiaceae* being sequenced, it will be of interest to determine what other members have this complex as well as the associated selenocysteine biosynthesis genes. The fact that these genes give rise to functional proteins that can affect the physiology of *S. meliloti* suggests that there must be some selective advantage to maintaining the genes. It may be noteworthy that all of our assays and growth were carried out aerobically, suggesting that FdoGHI also functions aerobically, in contrast to what is often found in many enteric bacteria.

It was previously thought that the presence of two formate dehydrogenase genes on pSymA might indicate that formate respiration was important within the nodule environment (7). Testing our formate dehydrogenase mutants carrying either a single, double, or triple mutation in any of the dehydrogenase genes did not show a visual symbiotic defect (data not shown). It may be that this region plays a role in allowing the bacteria to stay competitive within the rhizosphere, for example, by allowing them to withstand varying environmental conditions, such as water-saturated soils, which might lead to brief periods of hypoxia that would favor the accumulation of formate due to metabolic products from other organisms. Hypotheses such as these have not yet been addressed.

Our work on formate utilization and the demonstration of formate-dependent autotrophic growth has revealed an area of

metabolism and physiology that had not been previously recognized in *S. meliloti* at the molecular level. The questions that this work raises concerning the regulation of these determinants, as well the physiological roles they play in the rhizosphere, are unanswered. Ongoing work in these areas should provide answers that will allow us to better understand the physiology of the agronomically important soil bacterium *S. meliloti*.

ACKNOWLEDGMENTS

We thank R. Sparling for advice concerning medium formulation and for the kind gifts of labeled bicarbonate and formate. We also thank Michelle Sille for the construction of pMM22.

This work was funded by an NSERC Discovery grant to I.J.O.

REFERENCES

1. **Abaibou, H., J. Pommier, S. Benoit, G. Giordano, and M. A. Mandrand-Berthelot.** 1995. Expression and characterization of the *Escherichia coli fdo* locus and a possible physiological role for the aerobic formate dehydrogenase. J. Bacteriol. **177:**7141–7149.
2. **Alexeyev, M.** 1999. The pKNOCK series of broad-host-range mobilizable suicide vectors for gene knockout and targeted DNA insertion into the chromosome of gram-negative bacteria. BioTechniques. **26:**824–828.
3. **Altschul, S. F., T. L. Madden, A. A. Schäffer, J. H. Zhang, Z. Zhang, W. Miller, and D. J. Lipman.** 1997. Gapped BLAST and PSI-BLAST: a new generation of protein database search programs. Nucleic Acids Res. **25:** 3389–3402.
4. **Baldani, J. I., R. W. Weaver, M. F. Hynes, and B. D. Eardly.** 1992. Utilization of carbon substrates, electrophoretic enzyme patterns, and symbiotic performance of plasmid-cured rhizobia. Appl. Environ. Microbiol. **58:**2308–2314.
5. **Bardin, S., S. Dan, M. Osteras, and T. M. Finan.** 1996. A phosphate transport system is required for symbiotic nitrogen fixation by *Rhizobium meliloti*. J. Bacteriol. **173:**4540–4547.
6. **Barnett, M. J., and R. F. Fisher.** 2006. Global gene expression in the rhizobial-legume symbiosis. Symbiosis **42:**1–24.
7. **Barnett, M. J., R. F. Fisher, T. Jones, C. Komp, A. P. Abola, F. Barloy-Hubler, L. Bowser, D. Capela, F. Galibert, J. Gouzy, M. Gurjal, A. Hong, L. Huizar, R. W. Hyman, D. Kahn, M. L. Kahn, S. Kalman, D. H. Keating, C. Palm, M. C. Peck, R. Surzycki, D. H. Wells, K. C. Yeh, R. W. Davis, N. A. Federspiel, and S. R. Long.** 2001. Nucleotide sequence and predicted functions of the entire *Sinorhizobium meliloti* pSymA megaplasmid. Proc. Natl. Acad. Sci. USA **98:**9883–9888.
8. **Beringer, J. E., J. L. Beynon, A. V. Buchanan-Wollason, and A. W. B. Johnston.** 1978. Transfer of the drug resistance transposon Tn*5* to *Rhizobium*. Nature **276:**633–634.
9. **Broughton, W. J., C. H. Wong, U. Lewin, U. Samrey, H. Myint, H. Meyer, D. N. Dowling, and R. Simon.** 1986. Identification of *Rhizobium* plasmid sequences involved in recognition of *Psophocarpus*, *Vigna*, and other legumes. J. Cell Biol. **102:**1173–1182.
10. **Casse, F., C. Boucher, J. S. Huillot, M. Michel, and J. Dénarié.** 1979. Identification and characterization of large plasmids in *Rhizobium meliloti* using agarose gel electrophoresis. J. Bacteriol. **113:**229–242.
11. **Charles, T. C., G. Q. Cai, and P. Aneja.** 1997. Megaplasmid and chromosomal loci for the PHB degradation pathway in *Rhizobium (Sinorhizobium) meliloti*. Genetics **146:**1211–1220.
12. **Charles, T. C., and T. M. Finan.** 1991. Analysis of a 1600-kilobase *Rhizobium meliloti* megaplasmid using defined deletions generated *in vivo*. Genetics **127:**5–20.
13. **Charles, T. C., R. S. Singh, and T. M. Finan.** 1990. Lactose utilization and enzymes encoded in *Rhizobium meliloti*: implications for population studies. J. Gen. Microbiol. **136:**2497–2502.
14. **Clark, S. R. D., I. J. Oresnik, and M. F. Hynes.** 2001. RpoN of *Rhizobium leguminosarum* bv. *viciae* strain VF39SM plays a central role in FnrN-dependent microaerobic regulation of genes involved in nitrogen fixation. Mol. Gen. Genet. **264:**623–633.
15. **Cowie, A., J. Cheng, C. D. Sibley, Y. Fong, R. Zaheer, C. L. Patten, R. M. Morton, B. Golding, and T. M. Finan.** 2006. An integrated approach to functional genomics: construction of a novel reporter gene fusion library for *Sinorhizobium meliloti*. Appl. Environ. Microbiol. **72:**7156–7167.
16. **Dunn, M. F.** 1998. Tricarboxylic acid cycle and anapleurotic enzymes in rhizobia. Fems Microbiol. Rev. **22:**105–123.
17. **Eardly, B. D., L. A. Materon, N. H. Smith, D. A. Johnson, M. D. Rumbaugh, and R. K. Selander.** 1990. Genetic structure of natural population of the nitrogen-fixing bacterium *Rhizobium meliloti*. Appl. Environ. Microbiol. **56:** 187–194.
18. **Enoch, H. G., and R. L. Lester.** 1975. The purification and properties of formate dehydrogenase and nitrate reductase from *Escherichia coli*. J. Biol. Chem. **250:**6693–6705.
19. **Felsenstein, J.** 1985. Confidence limits on phylogenies: an approach using the bootstrap. Evolution **39:**783–789.
20. **Felsenstein, J.** 2002. PHYLIP (Phylogeny Inference Package) version 3.6a. Department of Genetics, University of Washington, Seattle.
21. **Finan, T. M., E. Hartwieg, K. Lemieux, K. Bergman, G. C. Walker, and E. R. Signer.** 1984. General transduction in *Rhizobium meliloti*. J. Bacteriol. **159:** 120–124.
22. **Finan, T. M., B. Kunkel, G. F. de Vos, and E. R. Signer.** 1986. Second symbiotic megaplasmid in *Rhizobium meliloti* carrying exopolysaccharide and thiamine synthesis genes. J. Bacteriol. **167:**66–72.
23. **Finan, T. M., S. Weidner, K. Wong, J. Buhrmester, P. Chain, F. J. Vorholter, I. Hernández-Lucas, A. Becker, A. Cowie, J. Gouzy, B. Golding, and A. Pühler.** 2001. The complete sequence of the 1,683-kb pSymB megaplasmid from the N_2-fixing endosymbiont *S. meliloti*. Proc. Natl. Acad. Sci. USA **98:**9889–9894.
24. **Gage, D. J.** 2004. Infection and invasion of roots by symbiotic, nitrogen-fixing rhizobia during nodulation of temperate legumes. Microbiol. Mol. Biol. Rev. **68:**280–300.
25. **Galibert, F., T. M. Finan, S. R. Long, A. Pühler, P. Abola, F. Ampe, F. Barloy-Hubler, M. J. Barnett, A. Becker, P. Boistard, G. Bothe, M. Boutry, L. Bowser, J. Buhrmester, E. Cadieu, D. Capela, P. Chain, A. Cowie, R. W. Davis, S. Dréano, N. A. Federspiel, R. F. Fisher, S. Gloux, T. Godrie, A. Goffeau, B. Golding, J. Gouzy, M. Gurjal, I. Hernández-Lucas, A. Hong, L. Huizar, R. W. Hyman, T. Jones, D. Kahn, M. L. Kahn, S. Kalman, D. H. Keating, E. Kiss, C. Komp, V. Lelaure, D. Masuy, C. Palm, M. C. Peck, T. M. Pohl, D. Portetelle, B. Purnelle, U. Ramsperger, R. Surzycki, P. Thébault, M. Vandenbol, F. J. Vorhölter, S. Weidner, D. H. Wells, K. Wong, K. C. Yeh, and J. Batut.** 2001. The composite genome of the legume symbiont *Sinorhizobium meliloti*. Science **293:**668–672.
26. **Hanahan, D.** 1983. Studies on transformation of *Escherichia coli* with plasmids. J. Mol. Biol. **166:**557–570.
27. **Hanus, F. J., R. J. Maier, and H. J. Evans.** 1979. Autotrophic growth of H_2-uptake-positive strains of *Rhizobium japonicum* in an atmosphere supplied with hydrogen gas. Proc. Natl. Acad. Sci. USA **76:**1788–1792.
28. **House, B. L., M. W. Mortimer, and M. L. Kahn.** 2004. New recombination methods for *Sinorhizobium meliloti* genetics. Appl. Environ. Microbiol. **70:** 2806–2815.
29. **Jormakka, M., B. Byrne, and S. Iwata.** 2003. Formate dehydrogenase—a versatile enzyme in changing environments. Curr. Opin. Struct. Biol. **13:**418–423.
30. **Jormakka, M., B. Byrne, and S. Iwata.** 2003. Protonmotive force generation by a redox loop mechanism. FEBS Lett. **545:**25–30.
31. **Jormakka, M., S. Toronoth, B. Byrne, and S. Iwata.** 2002. Molecular basis of proton motive force generation: structure of formate dehydrogenase-N. Science **295:**1863–1868.
32. **Kaneko, T., Y. Nakamura, S. Sato, K. Minamisawa, T. Uchiumi, S. Sasamoto, A. Watanabe, K. Idesawa, M. Iriguchi, K. Kawashima, M. Kohara, M. Matsumoto, S. Shimpo, H. Tsuruoka, M. Yamada, and S. Tabata.** 2002. Complete genomic sequence of nitrogen-fixing symbiotic bacterium *Bradyrhizobium japonicum* USDA110. DNA Res. **9:**189–197.
33. **Keen, N. T., S. Tamaski, D. Kobayashi, and D. Trollinger.** 1988. Improved broad-host range plasmids for DNA cloning in gram-negative bacteria. Gene **70:**191–197.
34. **Lambert, G. R., M. A. Cantrell, F. J. Hanus, S. A. Russell, K. R. Hadad, and H. J. Evans.** 1985. Intra- and interspecies transfer and expression of *Rhizobium japonicum* hydrogen uptake genes and autotrophic growth capability. Proc. Natl. Acad. Sci. USA **82:**3232–3236.
35. **Latner, A. L., and A. W. Skillen.** 1968. Isoenzymes in biology and medicine. Academic Press, New York, NY.
36. **Lepo, J. E., F. J. Hanus, and H. J. Evans.** 1980. Chemoautotrophic growth of hydrogen-uptake-positive strains of *Rhizobium japonicum*. J. Bacteriol. **141:**664–670.
37. **Lodwig, E., and P. Poole.** 2003. Metabolism of *Rhizobium* bacteroids. Crit. Rev. Plant Sci. **22:**37–78.
38. **Lowe, R. H., and H. J. Evans.** 1962. Carbon dioxide requirement for growth of legume nodule bacteria. Soil Sci. **94:**351–356.
39. **Manian, S. S., and F. O'Gara.** 1982. Derepression of ribulose bisphosphate carboxylase activity in *Rhizobium meliloti*. FEMS Microbiol. Lett. **14:**95–99.
40. **Mauchline, T. H., J. E. Fowler, A. K. East, A. L. Sartor, A. H. F. Hosie, P. S. Poole, and T. M. Finan.** 2006. Mapping the *Sinorhizobium meliloti* 1021 solute-binding protein-dependent transportome. Proc. Natl. Acad. Sci. USA **103:**17933–17938.
41. **Meade, H. M., S. R. Long, G. B. Ruvkin, S. E. Brown, and F. M. R. Ausubel.** 1982. Physical and genetic characterization of symbiotic and auxotrophic mutants of *Rhizobium meliloti* induced by transposon Tn*5* mutagenesis. J. Bacteriol. **149:**114–122.
42. **Miller, J. H.** 1972. Experiments in molecular genetics. Cold Spring Harbor Laboratory, Cold Spring Harbor, NY.
43. **Omata, T., G. D. Price, M. R. Badger, M. Okamura, S. Gohta, and T. Ogawa.** 1999. Identification of an ATP-binding cassette transporter involved in bicarbonate uptake in the cyanobacterium *Synechoccus* sp. strain PCC 7942. Proc. Natl. Acad. Sci. USA **96:**13571–13576.

44. **Oresnik, I. J., and D. B. Layzell.** 1994. Composition and distribution of adenylates in soybean (*Glycine max* L.) nodule tissue. Plant Physiol. **104:** 217–225.
45. **Oresnik, I. J., S. L. Liu, C. K. Yost, and M. F. Hynes.** 2000. Megaplasmid pRme2011a of *Sinorhizobium meliloti* is not required for viability. J. Bacteriol. **182:**3582–3586.
46. **Oresnik, I. J., L. A. Pacarynuk, S. A. P. O'Brien, C. K. Yost, and M. F. Hynes.** 1998. Plasmid encoded catabolic genes in *Rhizobium leguminosarum* bv. *trifolii*: evidence for a plant-inducible rhamnose locus involved in competition for nodulation. Mol. Plant-Microbe Interact. **11:**1175–1185.
47. **Poysti, N. J., E. D. Loewen, Z. Wang, and I. J. Oresnik.** 2007. *Sinorhizobium meliloti* pSymB carries genes necessary for arabinose transport and catabolism. Microbiology **153:**727–736.
48. **Poysti, N. J., and I. J. Oresnik.** 2007. Characterization of *Sinorhizobium meliloti* triose phosphate isomerase genes. J. Bacteriol. **189:**3445–3451.
49. **Richardson, J. S., M. F. Hynes, and I. J. Oresnik.** 2004. A genetic locus necessary for rhamnose uptake and catabolism in *Rhizobium leguminosarum* bv. *trifolii*. J. Bacteriol. **186:**8433–8442.
50. **Richardson, J. S., and I. J. Oresnik.** 2007. L-Rhamnose transport in *Rhizobium leguminosarum* is dependent upon RhaK, a sugar kinase. J. Bacteriol. **189:**8437–8446.
51. **Sambrook, J., and D. W. Russell.** 2001. Molecular cloning: a laboratory manual, 3rd ed. Cold Spring Harbor Laboratory Press, Cold Spring Harbor, NY.
52. **Schroeder, B. K., B. L. House, M. W. Mortimer, S. N. Yurgel, S. C. Maloney, K. L. Ward, and M. L. Kahn.** 2005. Development of a functional genomics platform for *Sinorhizobium meliloti*: construction of an ORFeome. Appl. Environ. Microbiol. **71:**5858–5864.
53. **Selander, R. K., D. A. Caugant, H. Ochman, J. M. Musser, M. N. Gilmour, and T. S. Whittam.** 1986. Methods of multilocus enzyme electrophoresis for bacterial population genetics and systematics. Appl. Environ. Microbiol. **51:**873–884.
54. **Simon, R., U. Priefer, and A. Pühler.** 1983. A broad host range mobilization system for *in vivo* engineering: transposon mutagenesis in gram-negative bacteria. BioTechniques **1:**784–791.
55. **Spaink, H. P.** 2000. Root nodulation and infection factors produced by rhizobial bacteria. Annu. Rev. Microbiol. **54:**257–288.
56. **Stoschek, C. M.** 1990. Quantitation of protein. Methods Enzymol. **182:**50–68.
57. **Thompson, J. D., T. J. Gibson, F. Plewniak, F. Jeanmougin, and D. G. Higgins.** 1997. The CLUSTAL-X windows interface: flexible strategies for multiple sequence alignment aided by quality analysis tools. Nucleic Acids Res. **25:**4876–4882.
58. **Turner, R. J., A. L. Papish, and F. Sargent.** 2004. Sequence analysis of bacterial redox enzyme maturation proteins (REMPs). Can. J. Microbiol. **50:**225–238.
59. **Vincent, J. M.** 1970. A manual for the practical study of root nodule bacteria. Blackwell Scientific, Oxford, United Kingdom.
60. **Watson, R. J., R. Heys, T. Martin, and M. Savard.** 2001. *Sinorhizobium meliloti* cells require biotin and either cobalt or methionine for growth. Appl. Environ. Microbiol. **67:**3767–3770.
61. **Yost, C. K., A. M. Rath, T. C. Noel, and M. F. Hynes.** 2006. Characterization of genes involved in erythritol catabolism in *Rhizobium leguminosarum* bv. *viciae*. Microbiology **152:**2061–2074.